Shear Behavior of 3D Printed Stochastic Rock Discontinuities

Amirhossein Medghalchi and Bing Q. Li[(✉)]

Department of Civil and Environmental Engineering, Western University, London, ON, Canada
`bing.li@uwo.ca`

Abstract. Discontinuities have a significant impact on the geomechanical behaviour of rock masses and corresponding implications across rock engineering applications. The design, construction, safety, and stability analysis of rock masses are all based on the measurement of mechanical characteristics. Unfortunately, it is impossible to determine the uncertainty of a single discontinuity strength measurement since an individual specimen can only be tested once before it accumulates damage. This limitation can be addressed by recent advancements in 3D printing (3DP) technology to create multiple artificial discontinuity specimens with exactly the same geometry. In this study, we create molds utilising 3D printing technology, which allows us to cast discontinuity specimens using high-strength and brittle cement-based materials with mechanical properties close to rocks. These specimens are then tested in a Direct Simple Shear device. Specimens were not printed directly because there does not exist a 3DP material that can meet the requirements for high strength, high brittleness, and low ductility. We present uncertainty estimates for peak and residual friction angles at five values of JRC (Joint Roughness Coefficient) simulated using Gaussian random fields.

1 Introduction

Rock mass stability and seepage are greatly influenced by the numerous discontinuities present in natural rock masses. Geology and mechanics are combined in the field of rock mechanics, which examines how rock masses react to stress and pore pressure changes resulting from natural processes such as volcanism or tectonics, or anthropogenic activities such as excavation.

Numerous engineering specialties, including mining, civil, hydraulic, petroleum, subterranean, and geological engineering, also include rock mechanics as a foundational subject. Therefore, a large investment in rock mechanics research is required in these sectors to understand and forecast the mechanical behaviours of engineering rock masses. The impact of structural planes on the process of rock strength failure can be readily seen during laboratory experiments. The mechanical properties of a rock mass can be determined through these laboratory tests, and these parameters are crucial for further numerical simulations and engineering studies.

1.1 Discontinuities

The behaviour of rock masses can be dependent on the behavior of its discontinuities, which refers to any separation in the rock continuum that has effectively zero tensile strength. Discontinuities can be the most significant issue in a project, affecting the permeability, strength, and deformability of the rock mass. Additionally, any surface or underground excavation's stability could be severely impacted by a persistent discontinuity. For these reasons, it is crucial to gain a complete understanding of discontinuities' geometrical, mechanical, and hydrological characteristics as well as how they impact rock mechanics and, ultimately, rock engineering.

The term "roughness" refers to a discontinuity surface's departure from perfect planarity, and it can quickly escalate into a challenging mathematical process when three-dimensional surface characterisation methods such as polynomials, Fourier series, noise waveforms, or fractals are applied (Liu et al., 2022). Some popular methods focus on the distribution of apparent dip on the surface (Tatone and Grasselli, 2010) and Z_2 (Tse and Cruden, 1979). From a practical standpoint, only one technique—joint roughness—has any degree of universality. Coefficient **(JRC)**, which Barton and Choubey created (1977). With this technique, the roughness is quantified by comparing the profile of a discontinuity surface to a standard roughness profile.

1.2 3D Printing of Simulated Rocks

The most effective method for determining the mechanical properties of rocks has been laboratory testing since it allows researchers to see how rock mass specimens behave mechanically under various boundary conditions and observe key phenomena such as strength, deformation, and failure. Unfortunately, perfectly identical rock specimens cannot be created or examined twice, and thus the outcomes and conclusions may not be accurate representations of the inherent heterogeneity in rocks. Therefore, it is not possible to determine the inherent variability in mechanical characteristics of a rock mass without including some degree of its heterogeneity.

Therefore, the key to conducting laboratory testing is the reproduceable production of structurally complex specimens. Recently, three-dimensional printing (3DP) technology has been investigated and applied to the field of rock mechanics. To some extent, this method addresses problems like the preparation of identical specimens or the visualisation of the interior of intact rocks, opening up new possibilities for the study of rock mechanics. These techniques allow internal features such as cracks and mineralogy to be reproduced through a digital model. They can thus replace the conventional artificial vision estimates in the field of rock engineering. According to some test results, loading experiments on these 3D-printed materials mimic the process of rock sample failure, and their test curves resemble those of natural rock. However, due to the plastic and resin materials utilised, some physical and mechanical features of these 3D printed samples are very different from those of the rock mass, such as the density and failure characteristics. Particularly, the influence of a printed structural plane on the total strength of a rock mass model cannot be accurately captured. The strength of the "rock" in a 3D-printed rock mass model is typically lower than the strength of genuine rock, yet the "joint" is stronger than a real rock mass joint, which impacts the model's failure process during

testing. Accordingly, the applications and advancement of the use of 3DP technology in the rock mass are reviewed from the perspectives of materials, equipment, and test methods on the basis of 3DP technology in complex structural rock mass reconstruction and mechanical testing. Therefore, we utilized 3DP in the creation of rock specimens and carried out test experiments to see whether printed specimens could be used in place of real rock specimens in investigations involving deformation and failure. We printed molds to indirectly model joined specimens using laboratory compressive and direct shearing tests to produce specimen with 5 different values of JRC (Joint Roughness Coefficient). Our preliminary experiments do not involve directly printing specimens with complex flawed structures since to our knowledge no 3D printed material currently meets matches the high strength, high brittleness, and low ductility of hard rocks.

1.3 Review of 3D Printed Rocks

Currently, photosensitive resin, gypsum, and self-made materials based on sandstone are the principal materials that can be employed for 3DP of rock mass structures. Many times, at least one or two of the mechanical and failure properties of genuine rocks can be found in the rock specimens made from these materials. For instance, before printing, photosensitive resin was a liquid substance. These materials can be used to create rock specimens that have excellent precision and strength. Nevertheless, the issues with ductility and low brittleness make extra treatment necessary (Gao et al., 2021). Gypsum-based 3D-printed specimens, for instance, exhibit considerable brittleness during the failure process, but their strength falls short of that of typical rocks (Jiang et al., 2020). The specimen of sandstone-based material is fragile, yet its strength is different from that of natural rocks (Jiang et al., 2015). One material that satisfies the needs of the natural rock masses can be modified to overcome the limits of 3DP materials regarding the mechanical and failure characteristics of rocks. For instance, high brittleness materials can be added to photosensitive resin to change it and give it high brittleness, low ductility, and high strength properties. However, it necessitates the interdisciplinary study of geotechnical, chemical, and other related fields.

2 Material and Methods

2.1 2D Profile Lines of the Physical Model

The shear strength of a rock mass is one of the most important factors affecting stability in rock mass engineering. In particular, the shear strength of a structural plane is the most important mechanical parameter that controls engineering stability in a jointed rock mass (Du, Hu, Hu, & Guo, 2011). Here, we produce simulated joints at five values of JRC (4, 8, 12, 16, 20) were for shear strength testing (Fig. 1).

2.2 Printing Methodology and Materials

In light of the issues with direct printing of rock-like materials, molds were first 3D printed from which rock-like specimens were casted using cement-based materials.

First, the surface topography of the artificial discontinuity surfaces were generated using a Gaussian random field using the Python package GSTools (Müller et al., 2022), which follows the methodology prescribed by (Heße et al., 2014). All surfaces are generated using a length scale of 3mm, and variance of 0.02, 0.12, 0.2, 0.32, and 0.48 mm^2 for JRC of 4, 8, 12, 16, 20 respectively (Fig. 1). Note that each specimen, even at the same JRC value, are independently stochastically generated to understand the inherent variability of surface roughness. The gridded (0.1 mm grid spacing) topography was exported to MeshLab to create surfaces between points and then into an STL format file that can be used by 3D printers. The stl file was then processed into slices and appropriate print parameters (layer thickness, fill ratio, output path) were selected for the printer. The mold was then printed layer-by-layer on the basis of the defined operating rules for the five types of the JRC (Figs. 2 and 3).

Finally, specimens were casted from the 3D printed molds using a PVC pipe. 75 mm x 150 mm cylindrical specimens were casted using the 212HB cement product from Sika. The cement was selected to meet the extrudability, fluidity, and constructability characteristics. Cement, silica sand, silica fume, fast-hardening cement, expansion agent, water, and additives make up most of this cementitious material. The main component of the rock-like substance is fine sand that has been joined by cement slurry. Hardener and silica fume increase the material's fluidity and stickiness and make it easier for it to be extruded from the print head. They also increase the material's elastic modulus,
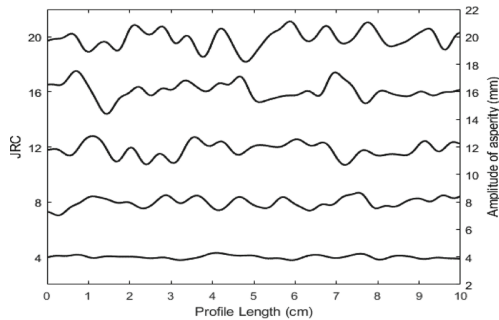

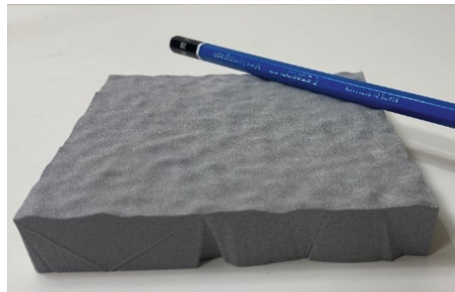**Fig. 1.** Example 2D cross sections
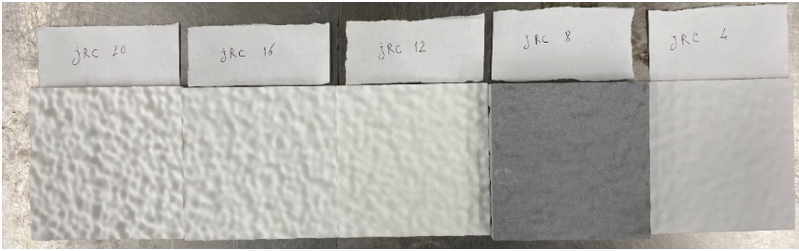

Fig. 2. Example of 3D printed mold

Fig. 3. 3D printed molds at all selected JRC values

lower the tension-to-compression ratio, and close the gap between cement mortar and rock. Cement that hardens rapidly makes construction of the material easier and speeds up the setting of the concrete. The 7-day compressive strength of this cement is 62 MPa.

2.3 Experimental Apparatus and Procedures

Shear experiments were conducted using the Western University direct shear machine as shown in Fig. 4.

The data logger sensor and data collection system were connected to the test machine, and the normal force, normal displacement, tangential force, and tangential displacement were recorded at 5 min-intervals. After the normal force was applied, shear displacement was applied at a rate of 0.00005 mm/min. We stopped shear tests when the either a) shear force decreased noticeably, indicating brittle shear failure, or b) when the shear stress reached a residual value. Specimens were tested at normal loads of either 20601 N or

Fig. 4. Simple shear apparatus with specimen in position

981 N, which is equivalent to a constant normal stress of either 466 kPa or 23 kPa. The two loads were considered to simulate a low overburden and an intermediate overburden.

3 Results

3.1 Load-Displacement Curves

Figures 5 and 6 show the shear test results of our artificial joints at different roughness and normal stress. Note that each specimen, even at the same JRC value, are uniquely stochastically generated to understand the inherent variability of surface roughness. The figures show that the shear process can be divided into 3 stages:

(1) The initial shear stage's gently curving slope indicates that the shear force affected the model gradually. With normal stress and shear stress, the upper and lower rock blocks moved toward one another, and under modest shear force, there was clear deformation. The structural plane was further compacted with increasing normal stress. Consequently, the initial shear step was cut short for greater normal stress.
(2) The stage of the shear increase, where the curvature was roughly linear. This is because when shear displacement increased, the shear stress increased quickly. Along with the increasing separation of the rock blocks on each side of the structural plane, the upper disc rose obliquely in the direction of the shear. During this phase, the stress fluctuated somewhat before finally stabilising under servo control.
(3) The stage of shear slip, during which the slope gradually flattened until it was approximately level. Typically, at this stage, the structural plane's maximum shear strength was reached. The shear strength of the structural plane then tended to stabilise or gradually deteriorate.

3.2 Description of Discontinuity Damage

All surfaces were painted prior to shearing. This paint is scratched during the shearing process, and images of selected post-shear specimens are shown in Fig. 7. It appears that both the size and quantity of damage patches increases with roughness from JRC = 4 to JRC = 12. The extent of damage is relatively consistent beyond JRC = 12. It also appears that the damage tends to occur at high-amplitude local maxima or minima, supporting the notion that the shear behaviour is controlled by the initial locking of these large asperities. We also note that the largest damage patches tend to locate near the center of the specimens, suggesting that the slip nucleates at the center of the specimens before propagating towards the specimen boundaries.

3.3 Peak and Residual Friction Angles

Figure 8 depicts the relation between JRC and friction angle, showing that both the peak and residual angles increase from JRC = 4 to JRC = 12, with minimal increase beyond JRC = 12. This reflects the damage patches shown in Fig. 7, suggesting that the contact and subsequent damage on specific asperities controls the shear strength of these discontinuities.
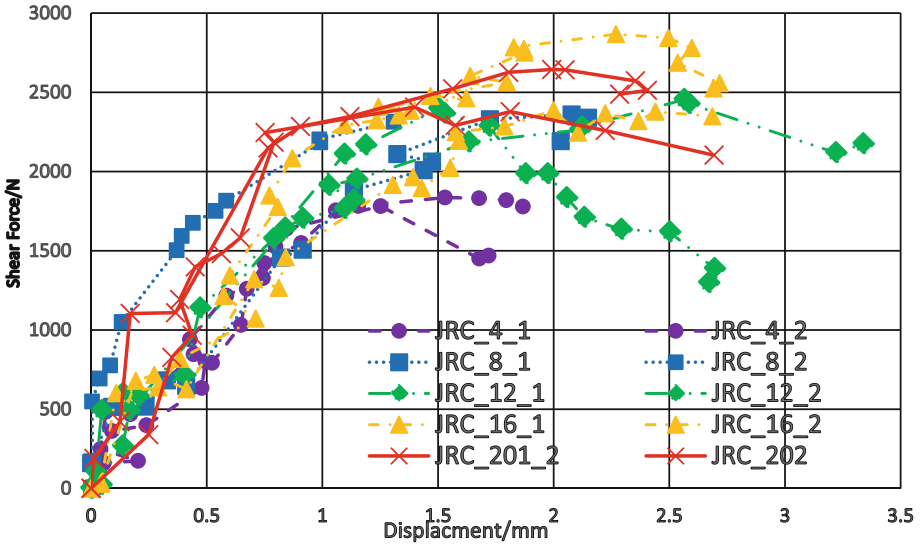
Fig. 5. Shear load-displacement curve of joints under 466 kPa normal stress
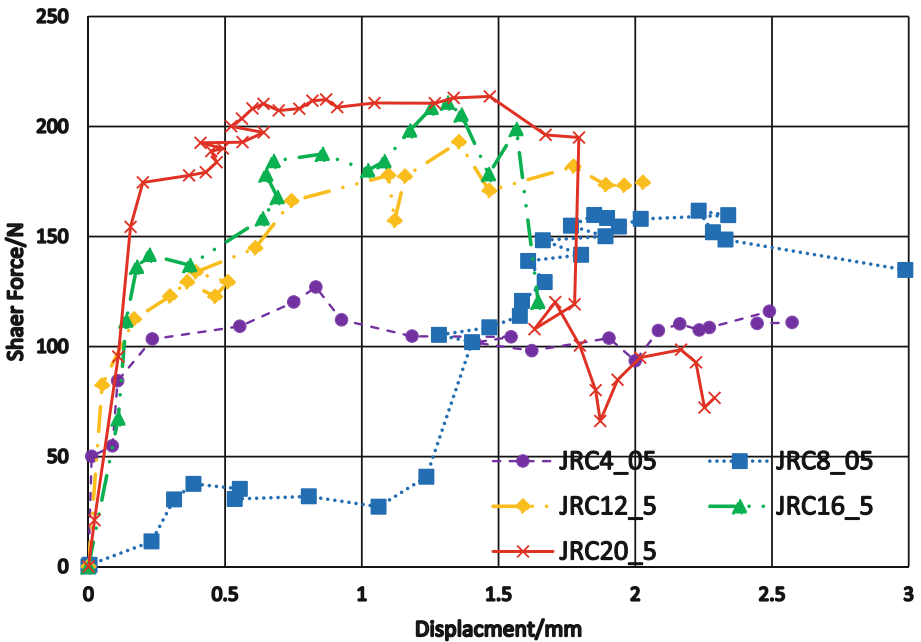

Fig. 6. Shear load-displacement curve of joints under 23 kPa normal stress.

Figure 9 shows the ratio of residual strength to peak strength at the tested roughness and normal stresses. This ratio appears to be relatively consistent except at low normal
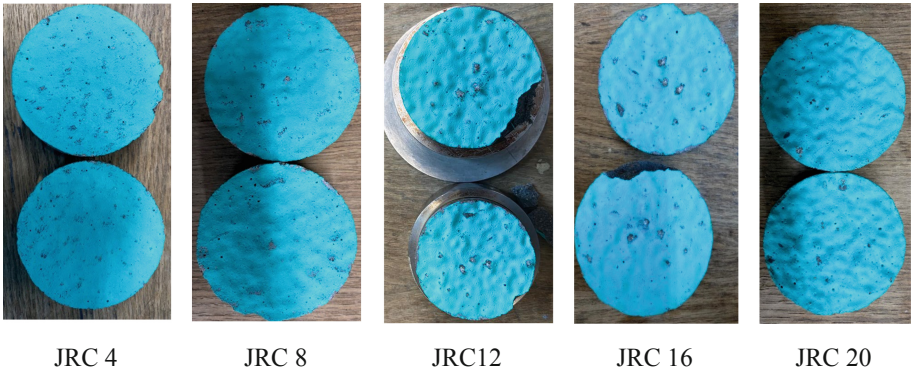
| JRC 4 | JRC 8 | JRC12 | JRC 16 | JRC 20 |

Fig. 7. Photos of specimens after shear testing at 466 kPa. Specimens were painted prior to shearing; grey areas indicate damage incurred during shearing.
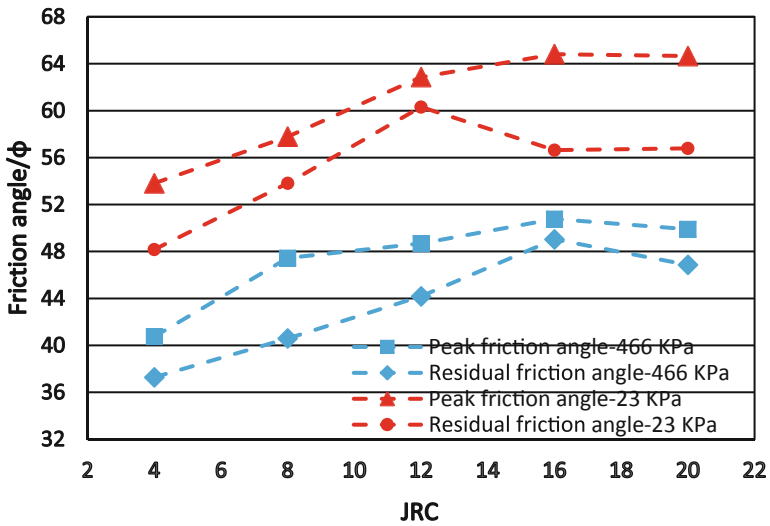
Fig. 8. Residual and Peak friction angle of model with various JRC

stress and high roughness where the residual strengths are significantly reduced. This may result from extensive brittle damage to the asperities as seen in the dramatic drops in shear forces shown in Fig. 6.

4   Discussion and Prospects

Conceptualized models can be easily and instantly transformed into physical models with 3D printing. Therefore, regardless of the difficulty of processing test samples, we can generate rock like specimens in specific forms and strengths for distinct experimental study purposes. It is possible to print rock-like specimens in a variety of shapes, including
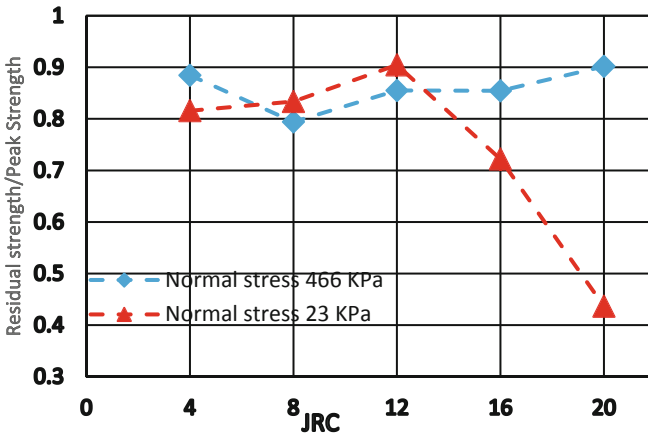
Fig. 9. Residual strength and peak strength of artificial joints over simulated JRC values.

cylinders, cuboids, and hollow cylinders. Additionally, they can be printed with unique local features including fractures, holes, interlayers, and seepage piping. The printed specimens can be utilised for a variety of experimental tests, including three-point bending, compressive testing, and tensile testing. Additionally, as printing materials and 3DP technology advance, these specimens can be produced with predetermined values for elasticity modulus, Poisson ratio, cohesion strength, and fractional angle by altering the mixed elements. Despite their obvious benefits, current 3DP approaches are still restricted in terms of experimental rock mechanics. Therefore, they should be improved and further developed to strengthen their function in geomechanically and geotechnical engineering. To make printed rock look like real rock, the printing medium must be improved. The capacity of 3DP technology to imitate rock-like materials with homogeneous strength is currently constrained by the availability of printing ingredients including sand powder, PLA, ABS, silicon rubber, glass-filled nylon, and metal powder. In order to print artificial rock-like specimens, it is necessary to investigate a new rock-like material with high compressive strength, low tensile strength, brittle failure, and frictional function. These short-term issues do not, however, negate the application potential of 3DP in the geotechnical area. In this study we 3D printed only negative molds and casted cement samples on these molds to circumvent these limitations. Therefore, we continue to have faith in its potential and believe that the drawbacks of 3DP technology can be overcome in the upcoming years and bring new insights into rock mechanics and engineering.

5   Conclusion

In this study, stochastically simulated rock discontinuity surfaces were manufactured using 3D printed negative molds and cement casting. These specimens were subjected to shear and uniaxial compression testing. The 3D printing procedure and mechanical tests led to the following conclusions:

1) The cementitious material printing method enables quick modification of the raw material ratio to adjust the material's mechanical properties such as elastic modulus, bulk density, and strength in comparison to conventional 3D printing techniques such as resin curing, plastic fused deposition, or powder bonded modelling. Cementitious materials are also brittle. As a result, the physical and mechanical characteristics of the 3D-printed cementitious material models or cast in situ material in printed mold are closer to those of genuine rocks.

2) A discontinuity's direct shear test under certain normal stresses demonstrates that the shear process may be separated into three stages. The peak shear strength of the structural plane steadily increases with increasing normal stress until JRC = 12, and remains consistent at higher roughness, along with the ratio of residual strength to peak strength. Additionally, in some circumstances, the ratio of residual strength to peak strength declines as discontinuity roughness increases. Qualitative observations of the damage patches also suggests that the shear slip nucleates near the center of the specimen and propagates outwards.

3) The results of these tests and printing technique show that synthetic rock specimens carry numerous benefits. The 3D-printed specimens have more reproducibility than actual rock samples, allowing the fabrication of comparable rock mass samples for various failure tests.

References

Barton, N., Choubey, V. (1977) The shear strength of rock joints in theory and practice. Rock Mech, 10:1–54.

Du, S., Hu, Y., Hu, X. and Guo, X. (2011) Comparison between empirical estimation by JRC-JCS model and direct shear test for joint shear strength. J Earth Sci, 22(3): 411–420.

Gao, M., Xie, J., Guo, J., Lu, Y., He, Z. and Li, C. (2021) Fractal evolution and connectivity characteristics of mining-induced crack networks in coal masses at different depths. Geomechanics and Geophysics for Geo-Energy and Geo-Resources, 7:1–15.

Jiang, L., Yoon, H., Bobet, A., Pyrak-Nolte, LJ (2020) Mineral Fabric as a Hidden Variable in Fracture Formation in Layered Media. Scientific Reports, 10: 2260

Quan Jiang, Xiating Feng, Lvbo Song, Yahua Gong,·Hong Zheng,·Jie Cui1 "Modeling rock specimens through 3D printing: Tentative experiments and prospects." Chinese Academy of Sciences and Springer-Verlag Berlin Heidelberg 2015

Liu, X., Zhu, W., Liu, Y., Guan, K. (2022) Reconstruction of rough rock joints: 2D profiles and 3D surfaces. International Journal of Rock Mechanics & Mining Sciences 156: 105113

Tatone BSA, Grasselli G (2010) A new 2D discontinuity roughness parameter and its correlation with JRC. Int J Rock Mech Min Sci 47(8):1391–1400

Tse R, Cruden DM (1979) Estimating joint roughness coefficients. Int J Rock Mech Min Sci 16(5):303–307

Heße, F., Prykhodko, V., Schlüter, S., Attinger, S. (2014) Generating random fields with a truncated power-law variogram: A comparison of several numerical methods. Environmental Modelling & Software, 55, 32–48

Müller, S., Schüler, L., Zech, A., and Heße, F. (2022) GSTools v1.3: a toolbox for geostatistical modelling in Python, Geosci. Model Dev., 15, 3161–3182, https://doi.org/https://doi.org/10.5194/gmd-15-3161-2022